

# Antiadhesive Role of Apical Decay-accelerating Factor (CD55) in Human Neutrophil Transmigration across Mucosal Epithelia

Donald W. Lawrence,<sup>1</sup> Walter J. Bruyninckx,<sup>1,2</sup> Nancy A. Louis,<sup>1</sup> Douglas M. Lublin,<sup>3</sup> Gregory L. Stahl,<sup>1</sup> Charles A. Parkos,<sup>4</sup> and Sean P. Colgan<sup>1</sup>

<sup>1</sup>Center for Experimental Therapeutics and Reperfusion Injury, Brigham and Women's Hospital, Harvard Medical School, Boston, MA 02115

<sup>2</sup>Department of Biology, Hanover College, Hanover, IN 47243

<sup>3</sup>Department of Pathology, Washington University School of Medicine, St. Louis, MO 63110

<sup>4</sup>Department of Pathology and Laboratory Medicine, Emory University School of Medicine, Atlanta, GA 30322

## Abstract

Neutrophil migration across mucosal epithelium during inflammatory episodes involves the precise orchestration of a number of cell surface molecules and signaling pathways. After successful migration to the apical epithelial surface, apically localized epithelial proteins may serve to retain PMN at the luminal surface. At present, identification of apical epithelial ligands and their PMN counter-receptors remain elusive. Therefore, to define the existence of apical epithelial cell surface proteins involved in PMN–epithelial interactions, we screened a panel of antibodies directed against epithelial plasma membranes. This strategy identified one antibody (OE-1) that both localized to the apical cell membrane and significantly inhibited PMN transmigration across epithelial monolayers. Microsequence analysis revealed that OE-1 recognized human decay-accelerating factor (DAF, CD55). DAF is a highly glycosylated, 70–80-kD, glycosyl-phosphatidylinositol-linked protein that functions predominantly as an inhibitor of autologous complement lysis. DAF suppression experiments using antisense oligonucleotides or RNA interference revealed that DAF may function as an antiadhesive molecule promoting the release of PMN from the luminal surface after transmigration. Similarly, peptides corresponding to the antigen recognition domain of OE-1 resulted in accumulation of PMN on the apical epithelial surface. The elucidation of DAF as an apical epithelial ligand for PMN provides a target for novel anti-inflammatory therapies directed at quelling unwanted inflammatory episodes.

Key words: mimetic • inflammation • endothelia • antibody • phage display

## Introduction

Neutrophils (PMN) are the first line of host defense against bacterial pathogens. The majority of pathogens are encountered at mucosal surfaces, and identification of pathways that elicit effective PMN mobilization to the epithelium has been an area of active investigation. To engage pathogens at sites of inflammation, PMN must first migrate out of circulation through the endothelial cell layer and into host tissue. Infections involving mucosal epithelial surfaces (intestine, lung, oral cavity) require that PMN migrate to epithelium in response to tissue-derived signals. Migration of PMN through epithelial barriers involves a concerted series of cell

surface crosstalk events between the PMN and epithelial cell. Evidence exists that initial PMN–epithelial binding requires PMN  $\beta_2$  integrins (especially CD11b/18; reference 1), and that subsequent movement of PMN through the paracellular space is dependent on epithelial CD47 interactions with PMN-expressed signal regulatory protein  $\alpha$  (Sirp $\alpha$ ; reference 2).

A critical site for PMN–pathogen interactions is the apical epithelial membrane, and this membrane domain represents

Address correspondence to Sean P. Colgan, Center for Experimental Therapeutics and Reperfusion Injury, Brigham and Women's Hospital, Harvard Medical School, 20 Shattuck St., Boston, MA 02115. Phone: (617) 278-0599; Fax: (617) 278-6957; email: colgan@zeus.bwh.harvard.edu

*Abbreviations used in this paper:* ANOVA, analysis of variance; CHO, Chinese hamster ovary; DAF, decay-accelerating factor; fMLP, *n*-formyl-methionyl-leucyl-phenylalanine; GPI, glycosyl-phosphatidylinositol; HMVEC, human microvascular endothelial cells; ICAM-1, intercellular adhesion molecule 1; PE-CAM, platelet-endothelial cell adhesion molecule; RFU, relative fluorescence units; SCR, short consensus repeats; Sirp $\alpha$ , signal regulatory protein  $\alpha$ .

the terminal stage for migrating PMN (1). Moreover, a histopathological hallmark of many mucosal inflammatory diseases is the formation of crypt abscesses, defined as the migration of large numbers of PMN across the apical epithelial surface and into the luminal aspect of the tissue (3). Such observations suggest that PMN utilize apical epithelial ligands to accomplish this task, yet apical ligands have not been studied in detail. Some evidence indicates that under certain circumstances (e.g., inflammatory bowel diseases), intercellular adhesion molecule 1 (ICAM-1) is expressed on the apical epithelial surface (4, 5) and can serve as an apical retention signal for PMN on the epithelium (5). Moreover, recent work has demonstrated that PMN Fc receptor binding to epithelial-bound antibody may contribute to the localization and retention of PMN on the apical membrane (6). At present, it is not known what molecular triggers might promote the dislocation of PMN from the epithelial surface.

Here, we sought to identify other apical epithelial ligands important in final stages of PMN transmigration. To do this, we screened a panel of monoclonal antibodies generated to epithelial plasma membrane antigen. This screen identified 1 mAb, termed OE-1, which recognized an apical epitope and inhibited physiologically directed PMN transmigration. Extensions of these observations identified the OE-1 antigen as decay-accelerating factor (DAF), a glycosyl-phosphatidylinositol (GPI)-link ~80-kD protein originally described as an inhibitor of autologous complement lysis (7). Subsequent studies revealed that DAF appears to function as an antiadhesive surface glycoprotein that regulates the rate of PMN migration across the apical epithelial membrane.

## Materials and Methods

**Cell Culture.** T84, Caco2, and KB cells were grown on permeable 0.33-cm<sup>2</sup> ring-supported polycarbonate filters (0.4- $\mu$ m pore size; Costar Corp.) or plastic polystyrene tissue culture dishes (Costar Corp.), as indicated, using techniques described previously (8–10). To plate inverted inserts, transwell inserts were placed upside down in a large petri dish and 80  $\mu$ l of cell suspension was plated on each insert. The inserts were incubated overnight at 37°C in a humidified incubator with 5% CO<sub>2</sub>. The following day, the inserts were flipped into DMEM supplemented with 20% FBS. Where indicated, human microvascular endothelial cells (HMVEC) were cultured as described previously (11). The nontransformed human oral keratinocyte cell line OKF6 was grown as described previously (12).

**Human Neutrophil Isolation.** PMN were freshly isolated from whole blood obtained by venipuncture from healthy human donors and anticoagulated with acid citrate dextrose as described previously (13). In brief, plasma and mononuclear cells were removed by aspiration from the buffy coat after centrifugation (400 g; 20 min) at room temperature. RBCs were sedimented using 2% gelatin, and residual RBCs were removed by lysis in ice-cold NH<sub>4</sub>Cl buffer. PMN were >90% pure as determined by microscopic evaluation. PMN were resuspended to a final concentration of  $5 \times 10^7$  in HBSS with 10 mM HEPES, pH 7.4, and without Ca<sup>2+</sup> or Mg<sup>2+</sup> (Sigma-Aldrich). PMN were used within 2 h of isolation.

**Monoclonal Antibody Production.** KB cell plasma membranes were used as an antigen to generate a panel of antibodies for functional screening. Plasma membranes were isolated using nitrogen cavitation (200 psi; 8 min; 4°C) as described previously (14). Mice were injected intraperitoneally with a 50:50 mix of TiterMax and KB membrane protein (50  $\mu$ g). Mice were inoculated every 2 wk for 6 wk with 25  $\mu$ g KB membranes in sterile PBS. Splenocytes were harvested, washed in PBS, and mixed 2:1 with hybridoma cells in the presence of 50% polyethyleneglycol. Cells were plated in DMEM supplemented with 1% HAT for selection. Single clones were obtained by limiting dilution (920 clones). Cultures of KB cells in 96-well plates were used in an ecto-ELISA to select for clones producing antibodies to epithelial surface proteins (510 clones). Supernatants from these clones were used in PMN transmigration assays to select for antibodies that inhibited transmigration by 50%. Of these, one antibody (subclone OE-1, IgG2a) was further characterized.

**Transmigration Assay.** PMN transmigration assays were performed as described previously (15). All epithelial experiments were performed in the physiologically relevant basolateral-to-apical direction (i.e., inverted monolayers), unless otherwise indicated, and all HMVEC transmigration studies were performed in the apical-to-basolateral direction. In brief, 10<sup>6</sup> PMN were added to the upper chambers of transwell inserts in which T84, KB, or Caco2 cell monolayers, as indicated, were plated on the opposing side. A chemotactic gradient was established by adding *n*-formyl-methionyl-leucyl-phenylalanine (fMLP) to the lower chambers (1  $\mu$ M for Caco2 and T84 epithelia; 10 nM for KB cells and HMVEC). PMN transmigration was performed at 37°C for 1 h with KB and HMVEC monolayers and for 2 h with T84 monolayers. Transmigrated PMN were quantified by assaying for the PMN azurophilic marker myeloperoxidase as described previously (16). In brief, transmigrated PMN were lysed by the addition of Triton X-100 to a final concentration of 0.5%. The samples were acidified with citrate buffer (final concentration 100 mM, pH 4.2). An aliquot of sample (70  $\mu$ l) was added to an equal volume of ABTS solution (1 mM ABTS [2,2'-azino-bis(3-ethylbenzo-thiazoline-6-sulfonic acid)], 0.03% H<sub>2</sub>O<sub>2</sub>, 100 mM sodium citrate buffer, pH 4.2) in a 96-well plate. The resulting color was quantitated on a plate reader at 405 nm. For kinetic transmigration and posttransmigration adhesion assays, monolayers were removed at the desired time point and placed in a new 24-well plate with HBSS and spun at 50 g for 5 min to dislodge PMN adherent to the monolayer (6). PMN were quantified by marker myeloperoxidase assay as described previously in this paragraph. Where indicated, polyclonal DAF antisera (a gift from B.P. Morgan, University of Wales, Cardiff, United Kingdom) or control polyclonal platelet-endothelial cell adhesion molecule (PE-CAM; a gift from J. Bischoff, Children's Hospital and Harvard Medical School, Boston, MA) antisera were used to assess transmigration.

**PMN Adhesion Assay.** PMN adhesion to confluent T84 epithelial cells was performed using modifications of a previous protocol (17). In brief, for studies of adhesion, human PMN were labeled for 30 min at 37°C with 2'-bis (carboxyethyl)-5 (6)-carboxyfluorescein pentaacetoxymethyl ester (BCECF-AM, 5  $\mu$ M final concentration; Calbiochem) and washed three times in HBSS. Epithelial monolayers grown on 24-well plates were preincubated with mAb OE-1 or control W6/32 at indicated concentrations for 10 min at 37°C. BCECF-labeled PMN ( $2 \times 10^6$ /monolayer) were added to washed epithelial monolayers containing 10 nM fMLP, plates were centrifuged at 150 g for 4 min to uniformly settle PMN, and adhesion was allowed for 10 min at

37°C. Monolayers were gently washed three times with HBSS, and fluorescence intensity (excitation, 485 nm; emission, 530 nm) was measured on a fluorescent plate reader (Cytofluor™ model 2300; Millipore). Adherent cell numbers were determined from standard curves generated by serial dilution of known PMN numbers diluted in HBSS. All data were normalized for background fluorescence by subtraction of fluorescence intensity of samples collected from monolayers incubated in buffer only, without addition of PMN.

**Tryptic Digestion and Identification of OE-1 Antigen.** Bulk Ag was purified from ~500 cm<sup>2</sup> of confluent KB plasma membranes using OE-1-coupled affinity column (CnBr-activated sepharose 4B; Pierce Chemical Co.) as described previously (13). Antigen was eluted at low pH (150 mM NaCl, 100 mM glycine/HCl, pH 2.5, containing 1% *n*-octylglucoside). The resulting eluant was pH-neutralized and resolved by SDS-PAGE, and bands were localized by Coomassie stain. The resulting ~80-kD band (~100 pmol) was extracted and submitted to the Dana Farber Cancer Institute Peptide Core Facility for trypsin digestion and microsequence analysis.

**Immunofluorescent Staining of Epithelial Monolayers.** Caco2 cells were grown to confluency on membrane permeable filters. After transmigration, the inserts were fixed for 10 min at room temperature in 1% paraformaldehyde in cacodylate buffer (0.1 M sodium cacodylate, pH 7.4, 0.72% sucrose). After washing once with PBS, the cells were stained for 1 h at room temperature with a 130-μg/ml monoclonal OE-1, polyclonal anti-DAF (1:100), or monoclonal anti-CD11b (60 μg/ml; clone 44a). After washing twice in PBS, the monolayers were incubated with either 1 μg/ml goat anti-mouse Oregon green or 1 μg/ml goat anti-rabbit Texas red. Fluorescent secondary antibodies were purchased from Molecular Probes. Stained inserts were carefully excised and mounted in polyvinyl alcohol mounting media. Laser Sharp imaging software (Bio-Rad Laboratories) was used for confocal imaging and processing.

**Immunoblotting Experiments.** Indicated cells were grown to confluency on 100 mm plastic petri dishes. The monolayers were lysed for 10 min in 1 ml lysis buffer (150 mM NaCl, 25 mM Tris, pH 8.0, 5 mM EDTA, 2% *n*-octylglucoside, and 10% mammalian tissue protease inhibitor cocktail; Sigma-Aldrich), scraped, and collected into microfuge tubes. After spinning at 14,000 *g* to remove cell debris, the pellet was discarded. Proteins were solubilized in nonreducing Laemmli sample buffer and heated to 100°C for 5 min. Samples were resolved on a 10% polyacrylamide gel and transferred to nitrocellulose membranes. The membranes were blocked 1 h at room temperature in PBS supplemented with 0.2% Tween 20 (PBS-T) and 4% BSA. The membranes were incubated in 3 μg/ml OE-1 in PBS-T for 1 h at room temperature, followed by 10-min washes in PBS-T. The membranes were incubated in 1:10,000 goat anti-mouse IgG (ICN/Cappel) and conjugated to horseradish peroxidase for 1 h at room temperature. The wash was repeated, and proteins were detected by enhanced chemiluminescence.

**Sequential Immunoprecipitations.** Cells were grown to confluency on 100 mm plastic petri dishes. The monolayers were lysed with 1 ml lysis buffer. Cellular debris was removed by centrifugation, and the lysates were precleared with 25 μl of a 50% protein G-sepharose slurry (Amersham Biosciences) for 2 h at 4°C. 20 μg OE-1 or 20 μg polyclonal anti-DAF was added to 1 ml of lysate, rotated overnight at 4°C, and subjected to capture with 50 μl of 50% protein G-sepharose slurry. After the protein G-sepharose beads had been removed, the immunoprecipitation reaction was repeated two more times to effectively remove the OE-1 antigen.

Finally, OE-1 and anti-DAF immunoprecipitated lysates were subjected to a final immunoprecipitation reaction with anti-DAF or OE-1 antibody, respectively. The captured antigen from each immunoprecipitation reaction was washed three times in immunoprecipitation wash buffer. After solubilization in Laemmli sample buffer, protein were resolved by SDS-PAGE and visualized by Western blotting with OE-1.

**Differential Biotinylation of Apical and Basolateral Surface Proteins.** T84 cells were grown to confluence on 0.5 μm polycarbonate transwell inserts. The monolayers were washed once in HBSS. Sulfo-NHS-biotin (Pierce Chemical Co.) was diluted in HBSS to a final concentration of 1 mM and added apically or basolaterally for 10 min at 4°C. The monolayers were washed repeatedly with HBSS containing 150 mM NH<sub>4</sub>Cl to quench the residual biotin. Monolayers were lysed in lysis buffer for 10 min at 4°C. After removal of cellular debris by centrifugation, 20 μg OE-1 was added to immunoprecipitate DAF. Biotinylated cell surface DAF was detected with avidin-horseradish peroxidase (Pierce Chemical Co.).

**DAF Suppression Studies.** Caco2 cells were chosen for these experiments because they are more easily transfected than T84 cells. Confluent Caco2 monolayers were dislodged from T175 flasks with trypsin. Cells were washed once in serum-free DMEM. 100 μl serum-free media, 10 μl DAF siRNA ribonucleotide (20 μM each of sense 5'-AAUCCUGGCGAGAAG-GACUCdTdT-3' and antisense 3'-dTdTUUAAAGGACCGCU-CUCCUGAG-5', synthesized by Xeragon, Inc.), or 10 μl phosphorothioate derivatives of DAF antisense oligonucleotide (20 μM of 5'-CGTGTCTCAGAGACCGACTT-3', synthesized by Oligo's Etc.) was added. In both cases, a control oligonucleotide (5'-ATGGAGGGCGCCGGC-3') was used in parallel. To these solutions, 10 μl Superfect transfection reagent (QIAGEN) was added. The tubes were vortexed and incubated at room temperature for 10 min to allow transfection complexes formation. After this incubation, 400 μl of serum-containing media was added to the complexes, followed by 800 μl of cell suspension. The cells and complexes were mixed well and 80 μl of cell suspension was plated on the underside of each transwell insert. The inserts were incubated upside down overnight at 37°C in a humidified incubator containing 5% CO<sub>2</sub>. The following day, the inserts were flipped into DMEM-containing 20% FBS. Monolayers were used after 4 d of incubation.

**Phage Panning of OE-1.** The OE-1 binding epitope was analyzed using phage display (18). In brief, sepharose-coupled OE-1 was incubated with 20 μl aliquots of the random 9-mer LL9 phage library (~5 × 10<sup>10</sup> phage) in 1 ml HBSS containing 0.1% BSA (phage buffer) for 2 h at 4°C or for 1 h at 20°C in a 1.5-ml microcentrifuge tube as described previously (19). Antibody complexes were washed five times with phage buffer and bound phage were eluted for 5 min in 2 ml of 0.1 M glycine, pH 2.2, followed by the addition of phage buffer containing 0.5% Tween 20 to the remaining cell pellet. After neutralization with Tris buffer, pH 8.1, the titer of phage was determined in each fraction by plaque assay according to standard procedures. Phage elutes were amplified in "starved" K91 *Escherichia coli* on solid luria broth agar containing 75 μg/ml kanamycin, purified by precipitation with polyethylene glycol, and resuspended in 600 μl NaCl/Hepes buffer. An aliquot (20 μL) of purified phage was subsequently reapplied to a new aliquot of sepharose-coupled OE-1 for a total of three affinity purification and two amplification steps. Individual phage clones were isolated and amplified, and the random peptide sequences were deduced after sequencing the unique nucleotide region of the pIII protein. As a control

for OE-1-specific selection, parallel phage affinity purification steps were performed in a 1.5-ml microcentrifuge tube in the absence of OE-1, and a sample of the recovered phage was analyzed by sequencing of the DNA insert. Consensus sequence peptide (amino acid sequence EVEHWYRSG), as well as scrambled control peptide (amino acid sequence SPLAQAVRSSSR), was commercially synthesized (BioWorld Inc.) and tested in transmigration, and OE-1 binding assays were performed as described earlier in *Monoclonal Antibody Production*.

In subsets of experiments, peptides were biotinylated (sulfo-NHS-biotin; Pierce Chemical Co.), purified by reversed-phase HPLC, and tested for binding to PMN. In brief, PMN ( $10^7$  PMN in 1 ml) were incubated with biotinylated peptide DAF peptide or control peptide (each at 10  $\mu\text{g/ml}$ ) at 4°C for 1 h. PMN were washed three times in HBSS and incubated with rhodamine-labeled streptavidin (Roche Diagnostics). Samples were aliquoted on a 96-well plate, and fluorescence intensity (excitation, 550 nm; emission, 580 nm), expressed as relative fluorescence units (RFU), was measured on a fluorescent plate reader (Cytofluor™ model 2300; Millipore).

**Data Analysis.** PMN transmigration and ELISA data were compared by two-factor analysis of variance (ANOVA) or by Student's *t* test where appropriate. Values are expressed as the mean and SEM from at least three separate experiments.

## Results

**Fusion Results.** One fusion of splenocytes from mice immunized with KB cell membranes yielded 920 antibody-producing clones. Each clone was screened for reactivity to intact KB cells and for inhibition of PMN transmigration across KB cell monolayers. In total, 510 clones were epithelial-reactive and of these, 31 clones significantly influenced PMN transmigration ( $n = 29$  inhibited PMN migration >50%;  $n = 2$  promoted PMN migration >50%). Of these, one subclone (IgG2a, termed clone OE-1), which inhibited PMN migration in this screen, also bound dominantly to the apical cell surface (see *Biochemical Characterization of OE-1 Antigen*), and as such, was further characterized as an apical epithelial ligand for PMN.

**Functional Characterization of mAb OE-1.** OE-1 was tested on two epithelial cell lines (KB and T84 cells), and one nontransformed primary culture of HMVEC to determine the influence on PMN transmigration. As shown in Fig. 1, OE-1 significantly inhibited PMN migration in a concentration-dependent manner (for each,  $P < 0.025$  by ANOVA), with 3  $\mu\text{g/ml}$  inhibiting PMN transmigration by  $\geq 50\%$  compared with either no mAb ( $P < 0.001$ ) or to our binding control W6/32 directed against MHC class I ( $P < 0.01$ ; Fig. 1, A–C).

Recent works have suggested that PMN binding to epithelial bound antibody via surface Fc receptors may influence PMN trafficking through epithelia (6). To rule out the involvement of PMN Fc receptor ligation in this activity, we enzymatically cleaved OE-1 with papain to generate Fab fragments, and tested such Fab fragments for inhibition of PMN migration. As shown in Fig. 1 D, Fab fragments of OE-1 also inhibited PMN transmigration ( $P < 0.01$ ), indicating that such findings are not likely related to Fc-mediated interactions with PMN.

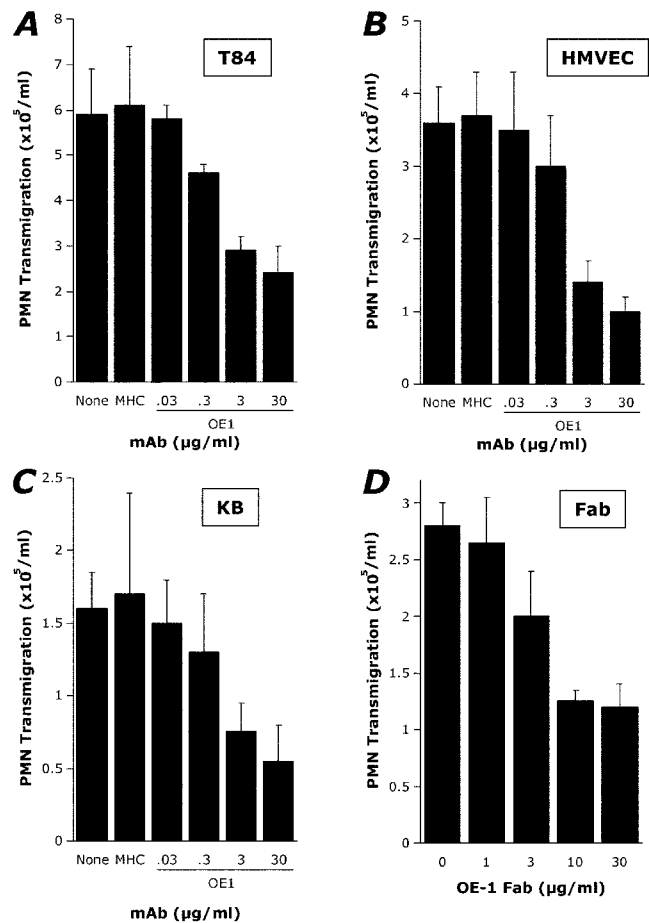


**Figure 1.** Functional influence of OE-1 on transmigration. Monoclonal antibody to epithelial surface protein inhibits human neutrophil transmigration. PMN migration across T84 monolayers (A, basolateral-to-apical direction), KB monolayers (B, basolateral-to-apical direction), or HMVEC monolayers (C, apical-to-basolateral direction) in response to a fMLP gradient was performed in the presence or absence of indicated concentrations of intact OE-1, control antibody (W6/32) or Fab fragments (D, KB cell transmigration, basolateral-to-apical direction). Data are presented as mean  $\pm$  SEM ( $n = 3$ ).

Previous papers have indicated that PMN transmigration across polarized epithelia can vary depending on the direction of migration (14, 15). As such, we examined whether OE-1 influenced PMN transmigration in a polarized fashion. Interestingly, inhibition of transmigration by OE-1 was independent of the direction of migration across electrically confluent ( $\text{TER} > 1,000 \Omega \cdot \text{cm}^2$ ), polarized T84 epithelia. Relative to 10  $\mu\text{g/ml}$  mAb control W6/32, 10  $\mu\text{g/ml}$  OE-1 inhibited PMN migration by  $69 \pm 8\%$  in the nonphysiologic apical-to-basolateral direction ( $P < 0.01$ ), and by  $73 \pm 10\%$  in the physiologically relevant basolateral-to-apical direction ( $P < 0.01$ ). In total, these results suggest that the OE-1 antigen represents a surface protein important to successful PMN transmigration across both endothelial and epithelial cell monolayers.

**Biochemical Characterization of OE-1 Antigen.** Next, we determined the relative nature and localization of OE-1 antigen. Confocal immunolocalization was used to determine

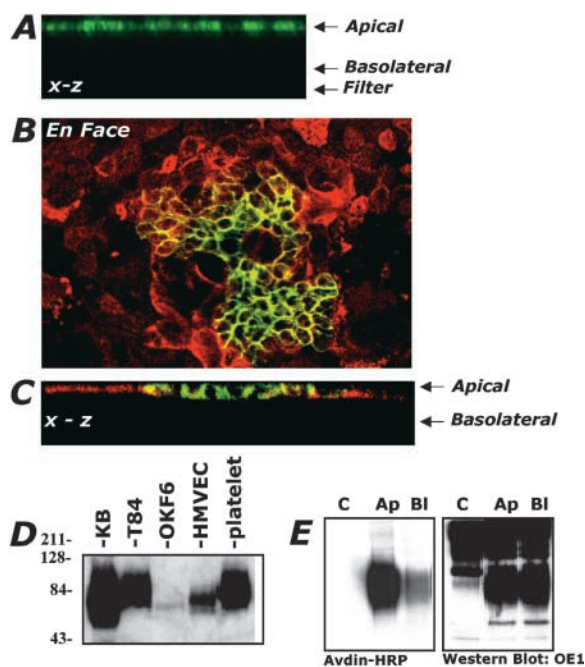


**Figure 2.** Localization of OE-1 antigen to the apical surface. (A) Confocal immunofluorescence was used to define the pattern of OE-1 antigen expression. Shown here is an x-z orientation series demonstrating nearly complete localization to the apical and subapical membrane compartment. (B) An apical confocal section localizing OE-1 (red) with the PMN marker CD11b/18 (clone 44a, green) after PMN transmigration. C represents an x-z orientation series of B. In D, equal amounts of lysates from indicated cell types were resolved on an 10% SDS-PAGE and immunoblotted with OE-1. The OE-1 antigen is expressed in varying amounts in the different cell types. The differences in molecular weights are likely due to differential glycosylation. Epithelial cell lines (KB, T84) express the highest levels of OE-1 antigen, followed by cells normally in close contact with complement proteins (HMVEC, platelets). Primary cell lines such as OKF6 (keratinocytes) express lesser amounts of the OE-1 antigen. (E) Confluent T84 monolayers were biotinylated on the apical (Ap) or basolateral (Bl) surface. Lysates were immunoprecipitated with either an isotype control antibody (C) or OE-1. Proteins were visualized with avidin-HRP to identify only surface, biotinylated DAF (left) or with OE-1 to demonstrate total DAF (right). Lanes labeled “C” represent isotype immunoprecipitation control samples.

the overall localization on T84 epithelia. As shown in Fig. 2 A, the OE-1 epitope localized exclusively to the apical membrane surface and to subapical membrane domains of polarized cells grown on membrane permeable supports. Localization of the antigen after PMN transmigration in the presence of OE-1 revealed that the OE-1 epitope remains localized to the apical domain and that PMN (localized with anti-CD11b mAb 44a) appear to “cluster” in distinct regions on the apical surface in the presence of OE-1 (Fig. 2, B and C). This clustering of PMN is consistent with previous observations (16), and is likely a result of localized epithelial barrier disruptions, with resultant increases in flux of chemoattractant.

Western blot analysis of the OE-1 epitope revealed a heavily glycosylated 70–80-kD protein expressed to varying degrees on a number of different cell types, including epithelial cells, endothelial cells, and platelets (Fig. 2 D).

The relatively small differences in apparent molecular weight between different cell lines likely represents cell tissue-specific differences in glycosylation (20). This antibody did not Western blot under reducing conditions (unpublished data). Immunoprecipitation of differential surface biotinylated T84 cells confirmed our confocal localization results, with nearly exclusive expression demonstrated in cells labeled from the apical, but not basolateral, surface (Fig. 2 E). Such results suggest that the OE-1 antigen represents a heavily glycosylated, ~70–80-kD protein expressed on the apical membrane surface.

**Identification of the OE-1 Antigen as DAF.** Next, experiments were performed to identify the antigen recognized by OE-1. Approximately 500 cm<sup>2</sup> of confluent KB cells were used to obtain sufficient quantities of OE-1 antigen for microsequence analysis. The antigen was digested with trypsin, and seven tryptic peptides resulting from mass spectroscopy showed direct sequence homology (Fig. 3 A) with CD55, also termed DAF, a glycoprotein organized into four homologous short consensus repeats (SCR, also

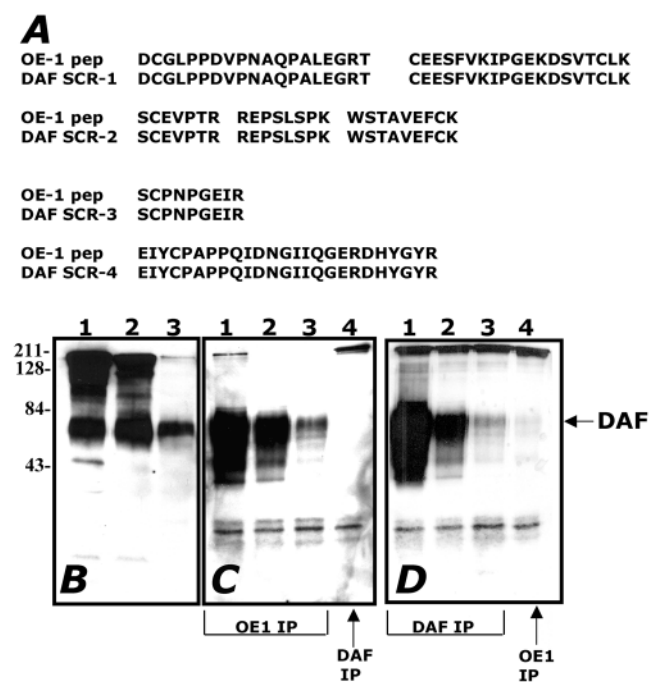


**Figure 3.** Biochemical identification of OE-1 antigen as human CD55; decay-accelerating factor (DAF). (A) Tryptic peptides derived from affinity-purified OE-1 antigen (OE-1 pep) aligned with DAF SCR domains 1–4. To confirm the identity of the OE-1 antigen as human CD55, IP reactions were performed. (B) T84 lysates were immunoprecipitated with OE-1 (lane 1) or a polyclonal anti-DAF (lane 2). The resolved proteins were immunoblotted using OE-1 under nonreducing conditions. Both antibodies immunoprecipitated identical proteins. Lane 3 is cell lysate run as a marker for DAF. (C) A single lysate was sequentially immunoprecipitated three times using 5 μl of anti-DAF per reaction. The captured protein from each IP reaction is shown in lanes 1–3. Note diminishing amounts of DAF recovered in each reaction. After the third reaction, the lysate was immunoprecipitated with 10 μg of OE-1 (lane 4). Lack of a recoverable protein confirms the identity of the OE-1 antigen as CD55. D is identical to the experiment in C, except the sequential IPs were first done using OE-1 and the final IP was done using polyclonal anti-DAF.

called complement control protein repeats) classically viewed as an inhibitor of autologous complement lysis (20). In support of this identification, and as suggested by our localization and Western blotting experiments (Fig. 2), DAF is a heavily glycosylated  $\sim 70$ – $80$ -kD protein widely expressed in many cells and tissue types. In addition, on most cell types, DAF exists predominantly as a GPI-anchored protein (20). In support of our apical localization results (Fig. 2), GPI-anchored proteins are predominantly expressed only on the apical membrane in polarized epithelial cells (21).

To further confirm the identity of DAF as the OE-1 antigen, we performed immunoprecipitation and immunodepletion experiments. As shown in Fig. 3 B, T84 lysates were immunoprecipitated with either OE-1 (lane 1), or polyclonal anti-DAF (lane 2). Lane 3 contains platelet lysate as a standard. As can be seen, both immunoprecipitation reactions pull down proteins of a similar molecular mass and degree of glycosylation. For the immunodepletion experiments, a single lysate was repeatedly immuno-

precipitated with OE-1 (Fig. 3 C), or polyclonal anti-DAF (Fig. 3 D). Each lysate was immunoprecipitated three times to deplete the antibody-binding protein, followed by a single immunoprecipitation with the opposing antibody (polyclonal anti-DAF or OE-1, respectively). As can be seen, the nearly complete absence of signal in the cross immunoprecipitation reactions (Fig. 3 C, lane 4 and Fig. 3 D, lane 4) confirmed that OE-1 and anti-DAF bind to identical antigens from epithelial lysates. Similarly, as shown in Fig. 4 A, polyclonal antisera against DAF, but not control antisera to PE-CAM, inhibited PMN transmigration in a concentration-dependent manner ( $P < 0.025$  by ANOVA). Together, these studies identify the OE-1 antigen as DAF and indicate that DAF is an apically localized epithelial protein that functions, at least in part, to modulate PMN migration.

*Apical DAF Represents an Antiadhesive PMN Ligand.* Next, we determined the functional role of epithelial DAF in modulation of PMN transmigration. We reasoned that if DAF is functional from the apical membrane surface of ep-

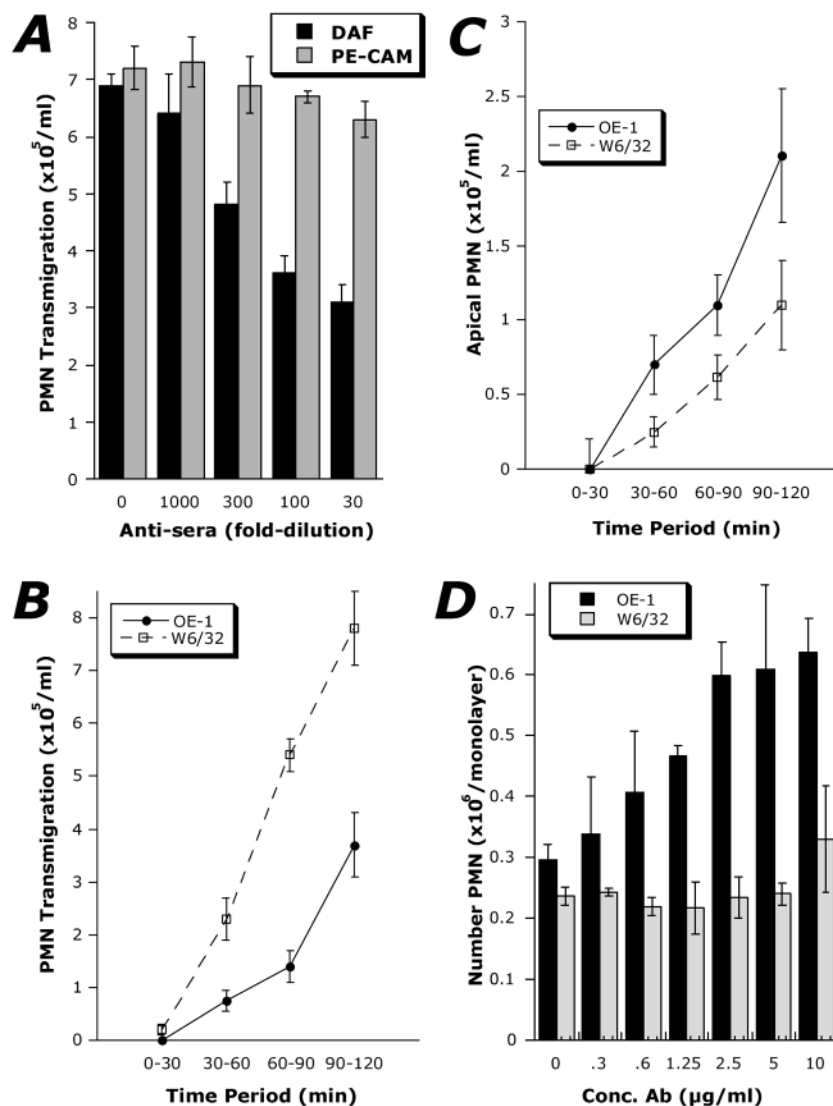


**Figure 4.** Role of DAF in the kinetics of PMN transmigration. (A) Influence of DAF antisera on PMN transepithelial migration. Epithelia were exposed to indicated concentrations of DAF (black bars) or control PE-CAM (shaded bars) antisera and assessed for PMN transmigration. (B and C) The influence of OE-1 (dashed line) or control W6/32 (solid line) on the kinetics of transmigration was assessed. B represents the number of PMN that completely traverse the epithelial monolayer and C represents the number of PMN that remain attached to the apical epithelial membrane. Data are presented as mean  $\pm$  SEM ( $n = 4$ ). (D) The influence of indicated concentrations of mAb OE-1 or control mAb W6/32 on fMLP-stimulated PMN adhesion to confluent T84 cells was assessed. Data are presented as mean  $\pm$  SEM ( $n = 4$ ).

ithelia, it may represent a terminal step in PMN migration, and as such, may contribute significantly to the kinetics of PMN accumulation at the apical membrane domain. Three approaches were used to define these principles. First, we examined the influence of OE-1 on the kinetics of PMN transmigration. To do this, we used an approach described previously that quantitates PMN migration from the same set of monolayers over blocks of time (6, 22). In our experiments, we assessed PMN every 30 min over a 2-h period. As shown in Fig. 4 B, compared with control W6/32, the presence of OE-1 significantly slowed PMN transmigration across T84 epithelial monolayers ( $P < 0.01$  by ANOVA). Significant differences were observed as early as 30–60 min, and were evident as late as 150 min (unpublished data). More importantly, this decrease in PMN transmigration shown in Fig. 4 B was almost completely explained by accumulation of PMN on the apical surface of epithelia (Fig. 4 C). Indeed, as early as 30–60 min, the number of apical PMN increased significantly in the presence of OE-1 ( $P < 0.05$  compared with W6/32) and remained elevated through the 120-min period. Such findings indicate that rather than inhibiting PMN transmigration, OE-1 promotes the apical accumulation of PMN on epithelia.

Second, we reasoned that if DAF functions as antiadhesive molecule, then OE-1 should promote adhesion to the apical surface of epithelia. To test this idea, epithelial-PMN adhesion assays were performed. As shown in Fig. 4 D, preincu-

bation of epithelia with increasing concentrations of OE-1 and determination of fMLP-stimulated PMN adhesion revealed that OE-1 increases PMN adhesion in a concentration-dependent fashion ( $P < 0.025$  by ANOVA). Such findings were not related to Fc receptor-mediated adhesion, because isotype control antibodies (clone W6/32) resulted in no significant increase in adhesion ( $P =$  not significant).

As a third approach, we used antisense oligonucleotides and siRNA technologies to diminish surface expressed DAF and examined the kinetics of PMN migration across such monolayers of epithelia. As determined by immunoprecipitation of surface-biotinylated protein (Fig. 5 A), antisense oligonucleotides and siRNA decreased surface expressed DAF by  $68 \pm 10\%$  and  $63 \pm 12\%$  relative to oligonucleotide controls ( $n = 3$  determinations). Using cells treated in this manner, we assessed transmigration and apical PMN accumulation. As shown in Fig. 5 B, PMN transmigration across both antisense and siRNA exposed cells was significantly diminished relative to either mock-treated or oligonucleotide control-treated monolayers ( $P < 0.025$  for both by ANOVA). Diminished PMN transmigration in DAF-depleted cells was less obvious when measured at early time points, and became most apparent beyond 90 min. Conversely, as shown in Fig. 5 C, assessment of apical PMN in DAF-depleted epithelia revealed a significant increase over time in a manner similar to mAb OE-1 exposure ( $P < 0.05$  for both by ANOVA). In addition, we

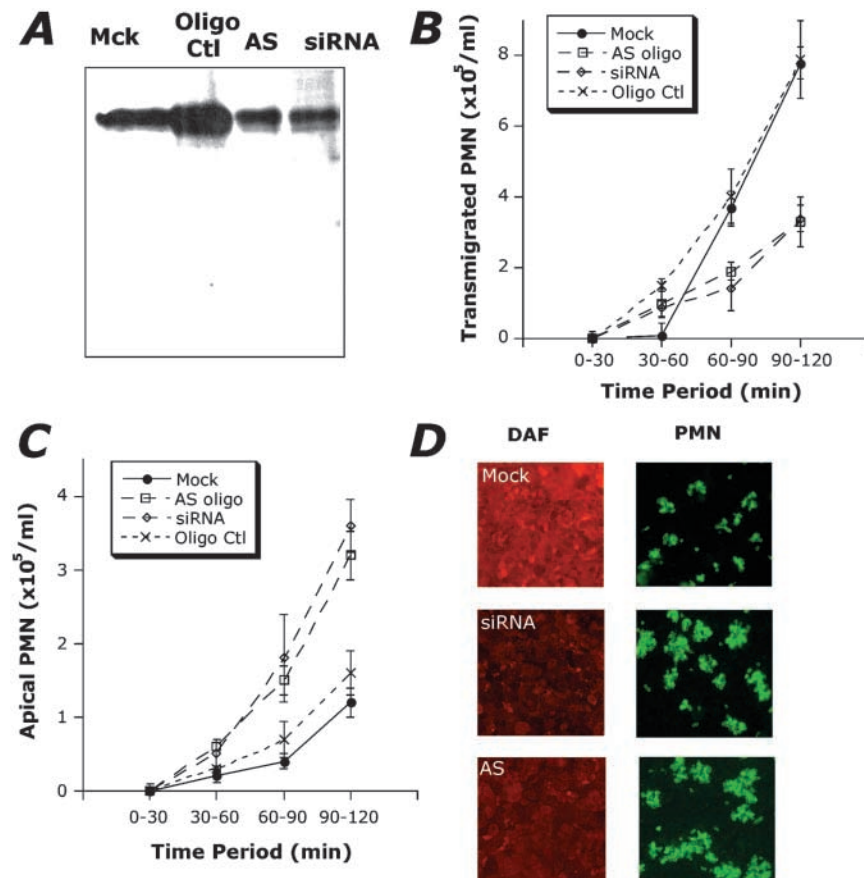


**Figure 5.** Influence of DAF depletion on PMN transmigration. (A) Representative Western blot analysis of total cellular DAF protein in Caco2 cells exposed to mock conditions (transfection loading reagent only), control oligonucleotide, DAF antisense oligonucleotide, or DAF siRNA. (B and C) The influence of siRNA (diamonds) and antisense oligonucleotide (squares) on the kinetics of transmigration was assessed. B represents the number of PMN that completely traverse the epithelial monolayer and C represents the number of PMN that remain attached to the apical epithelial membrane. Also shown are mock conditions (closed circles) and oligonucleotide control conditions (crosses). Data are presented as mean  $\pm$  SEM ( $n = 4$ ). (D) Immunofluorescence photomicrographs of PMN (green, localization of CD11b/18 with 44a) at the epithelial apical surface after transmigration in monolayers loaded with siRNA, antisense oligonucleotide (AS), or mock treatment. Decreased DAF expression (red, localization with OE-1) is associated with increased PMN clustering on the apical surface of epithelia (compare density of clusters in mock vs. siRNA/AS conditions).

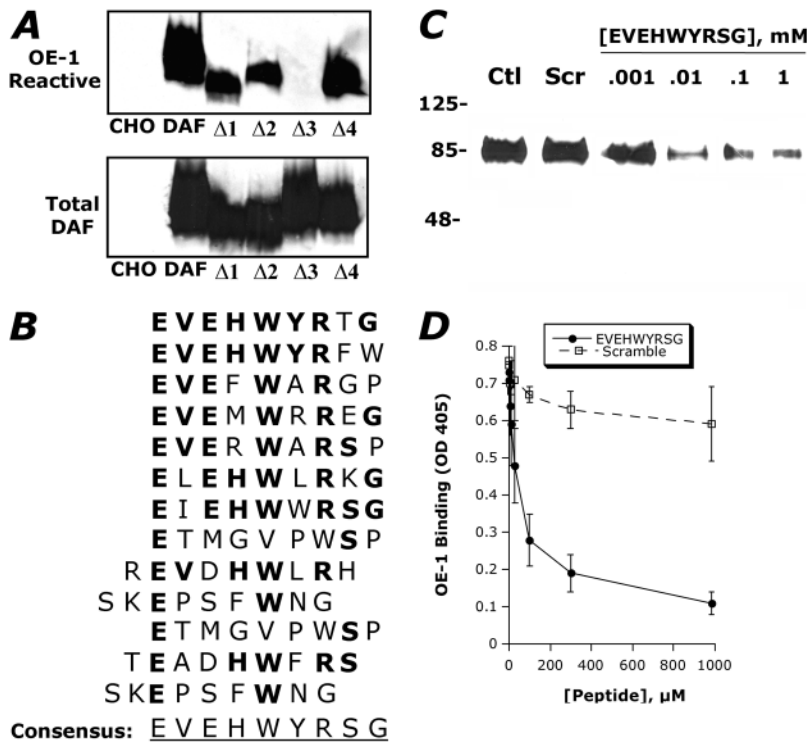


**Figure 6.** SCR domain mapping and identification of OE-1 epitope. (A) Lysates from CHO cell mutants expressing DAF with individual SCR domains deleted were used to map which SCR domain contained the OE-1 epitope. Lysates were resolved by SDS-PAGE and immunoblotted with OE-1 (top) or polyclonal DAF antisera (bottom) to assess total DAF. (lanes) CHO, unaltered CHO cells; DAF, CHO cells expressing full length DAF; Δ1–4, CHO cells expressing DAF with the corresponding SCR domain deleted. OE-1 does not recognize SCR-3 domain deletion. B represents 13 phage sequences and an overall consensus sequence eluted from three rounds of panning with OE-1–coupled sepharose. (B and C) OE-1 mAb was incubated with indicated concentrations of synthetic EVEHWYRSG peptide, or a control scrambled peptide (Scr), and used to probe Western blots from T84 epithelial lysates (C) or cell surface ELISA on intact T84 cells. Data are presented as mean  $\pm$  SEM ( $n = 3$ ).

determined whether it was possible to distinguish such biochemical differences at the morphological level. As shown in Fig. 5 D, confocal localization of PMN in mock and antisense/siRNA-treated monolayers after transmigration revealed increased PMN represented as large aggregations of PMN particularly prominent on the apical surface of DAF-depleted epithelia. Together, these results support our findings with mAb OE-1 and suggest that DAF represents an apically localized, antiadhesive PMN ligand that significantly influences the kinetics of PMN trafficking through epithelial monolayers.

**Phage Display Mapping of the OE-1 Binding Epitope.** Next, we extended these findings to determine the OE-1–binding epitope. Initially, we used OE-1–based Western blotting to screen Chinese hamster ovary (CHO) transfectants expressing wild-type human DAF and truncations of DAF SCR domains 1–4, as described previously (23). As shown in Fig. 6 A, these studies revealed the loss of OE-1 reactivity in only the SCR-3 truncation. Loss of SCR-3 was not due to diminished overall DAF expression, as determined by blotting of total DAF content using polyclonal anti-DAF antisera. Such findings suggest that OE-1 recognizes an epitope encoded, at least in part, by the SCR-3 domain of DAF.

To better define the DAF epitope recognized by OE-1, we used the LL9 phage library characterized previously displaying linear 9-mer peptides to select for OE-1 binding epitopes (19). The library underwent three rounds of panning over bound OE-1 with intermediate amplifications. The round 3–enriched phage had a titer of  $5.0 \times 10^9$  PFU/ml and yielded an enrichment of  $>3$  logs relative to round 1. As shown in Fig. 6 B, 13 phage clones were se-

quenced; aligned sequences revealed a number of structural similarities. In particular, a pattern amino acid sequence of EXEX\*WXXX\*\* (where X is neutral, X\* is large, and X\*\* is hydrophobic) emerged as a relatively close consensus match. Based on our analysis of DAF, and consistent with our observations that OE-1 does not Western blot under reducing conditions, this linear sequence did not exist in SCR domain 3. These findings suggest that OE-1 recognizes a nonlinear constrained epitope where, at least in part, SCR-3 contributes to this binding.

As shown in Fig. 6, a synthetic peptide corresponding to a best-fit OE-1 epitope consensus (EVEHWYRSG), but not a scrambled peptide, blocked OE-1 binding to denatured protein (Fig. 6 C, Western blot) and to the intact epithelial cell surface protein (Fig. 6 D, ELISA) in a concentration-dependent manner, suggesting that this EVEHWYRSG peptide is at least a reasonable match for the OE-1 epitope. In its labeled form (biotin–EVEHWYRSG), binding to the surface of intact PMN was readily detectable (fluorescence intensity,  $2,188 \pm 383$  RFU,  $n = 4$ ) compared with either labeled control peptide (fluorescence intensity,  $81 \pm 12$  RFU,  $P < 0.01$  compared with biotin–EVEHWYRSG) or to unlabeled peptide (fluorescence intensity,  $33 \pm 6$  RFU,  $P < 0.01$  compared with biotin–EVEHWYRSG).

Next, we determined whether this synthetic peptide influenced the PMN transmigration and accumulation of PMN on the surface of epithelia after transmigration. As shown in Fig. 7, PMN and epithelial preexposure to increasing concentrations of EVEHWYRSG, but not scrambled peptide, resulted in both increased apical accumulation of PMN (Fig. 7 A,  $P < 0.025$  by ANOVA) and diminished PMN transmigration ( $P < 0.05$  by ANOVA). Such data

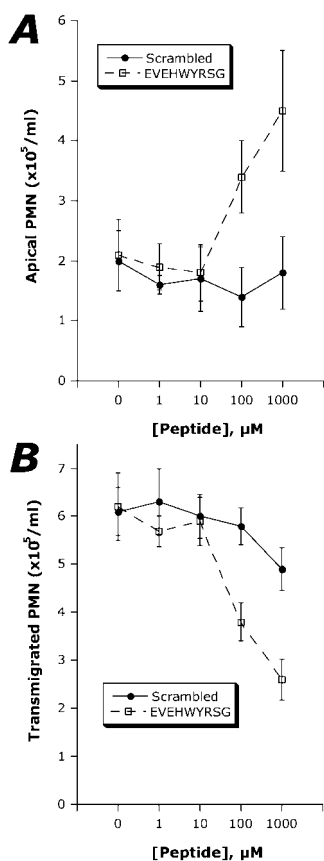


**Figure 7.** Influence of OE-1 peptide mimetic on the kinetics of PMN transmigration. PMN and the apical reservoir of epithelia were incubated with indicated peptides before coinubation and assessment of transmigration. (A and B) The influence of indicated concentrations of OE-1 peptide (EVEHWYRSG, dashed line), or a scrambled control (solid line), on the kinetics of transmigration was assessed. (A) The number of PMN that remain attached to the apical epithelial membrane is shown. (B) The number of PMN that completely traverse the epithelial monolayer is shown. Data are presented as mean  $\pm$  SEM ( $n = 3$ ).

support our OE-1 findings and suggest that we can recapitulate this biology with a closely matched synthetic mimetic corresponding to the OE-1 epitope.

## Discussion

Transepithelial migration of PMN is the pathological hallmark of active mucosal inflammation and occurs in such disease states as inflammatory bowel disease, periodontitis, cystitis, and infectious enterocolitis (24). Before movement through the interstitium to the epithelium, PMN first escape the vasculature through a distinct, well-characterized set of interactions with the endothelium. Less is known about leukocyte interactions with epithelial cells. We report here that CD55 represents an apical, antiadhesive ligand for PMN during transmigration.

The current paradigm for transmigration of PMN across epithelial monolayers envisions a process consisting of sequential molecularly defined events, including initial CD11b/18-mediated interactions of PMN with epithelia (24, 25). Unlike endothelial cells, a number of papers using diverse epithelial models have demonstrated that ICAM-1 is not an epithelial ligand for PMN  $\beta_2$  integrins (5, 15, 16, 26, 27), although under some conditions, ICAM-1 may function as an apical anchor for PMN (5). Functional mapping studies of this  $\beta_2$  integrin-dependent pathway have suggested that the profile of inhibition is distinct from that of other known ligands of CD11b/CD18 (28). Subsequent

CD47-mediated orchestration of PMN movement through the paracellular space is now a well-accepted principle (24). Apical ligands for PMN are less well understood, and for that reason, we sought to better define the existence of apical PMN ligands on epithelia. A monoclonal strategy was used that screened based on criteria as follows: (a) epithelial surface binding, (b) modulation of PMN migration, and (c) localization to the apical membrane. This strategy identified OE-1 and was demonstrated to bind and regulate PMN migration across diverse epithelial monolayers, including nontransformed cell types (e.g., HMVEC).

Immunopurification and microsequencing identified the OE-1 ligand as DAF. Although most analyses of DAF function have focused on inhibition of complement-mediated lysis, it is important to note that DAF also has non-complement ligands (29). For example, DAF is an established ligand for CD97 on leukocytes. Our studies here revealed that DAF functions to modulate the rate of PMN dislocation from the apical epithelial membrane, and as such, serves as an antiadhesive terminal step in the PMN transmigration process. Of note, some experiments indicated that mAb OE-1 also inhibited PMN transmigration in the nonphysiologic direction (apical-to-basolateral), and by inference, this observation suggests that DAF is a critical control point for movement of PMN through the paracellular space. These findings of DAF as an antiadhesive molecule are consistent with some previous observations in other models. For example, King et al. screened a panel of antibodies and concluded that DAF, among other surface molecules, functions to inhibit adhesion of T cells to macrophage-like cells (30). In a more physiologic context, Verbakel et al. demonstrated that human DAF expressed in the rat heart functioned effectively as an antiadhesive molecule (31). Clearly, this idea was supported by evidence that OE-1 promotes direct PMN-epithelial adhesion, and peptides representing the OE-1 epitope appear to promote PMN accumulation. The idea of antiadhesive molecules has not been widely studied, and surprisingly little is known about the de-adhesion state of integrins during the process of transmigration. Some evidence indicates that the major leukocyte sialoglycoprotein CD43 may function in de-adhesive interactions of leukocytes with parenchymal cells, and as such, may counterbalance a number of proadhesive integrin functions (30, 32–34). In addition, previous work has indicated that integrin avidity is both activatable and transient, thereby providing a cycle of adhesion and de-adhesion (35–37). Finally, elegant work in the past has indicated that calcineurin may critically regulate integrin binding to matrix components through transient control of intracellular  $Ca^{2+}$  levels (38).

The present findings indicate that DAF may regulate the overall kinetics of PMN movement through the epithelium. Of interest, the paracellular PMN ligand CD47 also functions in a kinetic manner. For example, it was shown recently that whereas monoclonal antibodies directed against CD47 delay transepithelial migration, with time, this anti-CD47 influence is overcome (22). Such surface CD47 function was linked to as yet undefined tyrosine

phosphorylation events, suggesting a critical kinetic signaling pathway influencing the rate of PMN migration. In addition, recent works suggest that transmembrane CD47 signaling function may function, at least in part, in concert with signal regulatory protein- $\alpha$  (SIRP $\alpha$ ), a cell surface protein containing three immunoglobulin superfamily domains and intracellular immunoreceptor tyrosine-based inhibitory motifs (39). CD47 is a ligand for Sirp $\alpha$  (40), and analyses have suggested that CD47 function is proportional to the expression of Sirp $\alpha$  and that Sirp $\alpha$  interactions with CD47 binding may mediate cell–cell interactions (40).

At present, we do not know the PMN ligand for epithelially expressed DAF. Results using biotinylated peptide corresponding to the OE-1 epitope readily bound to PMN (Results), suggesting that the OE-1-binding region in DAF is conformationally similar to a PMN binding site. As alluded to in a previous paragraph, a number of papers have indicated that CD97, a recently identified seven-span transmembrane (7-TM) protein expressed by a variety leukocytes early after activation, is a counter-receptor for DAF (41–43), and these interactions have been profiled in a number of diseases (44–46). Analyses of structure–function relationships have indicated that CD97–DAF interactions represent a Ca<sup>2+</sup>-dependent, low affinity interaction (47); that CD97 interacts with the NH<sub>2</sub> terminal SCR-1 domain on DAF (41); that at least three tandemly linked EGF domains on CD97 are necessary for DAF interactions (42); and that larger splice variants of CD97 (containing more than three EGF repeats) have a significantly lower affinity for DAF (42). Our attempts to block either PMN transmigration or apical clustering of PMN with functionally inhibitory anti-CD97 mAb (e.g., clone VIM3b) in this model have not resulted in differences compared with control antibodies (unpublished data). A number of important considerations may contribute to the lack of influence of anti-CD97 in our model. First, CD97–DAF may be a low enough affinity that we are not able to detect the relative importance of CD97 within our system. Second, it is possible that accessory molecules not expressed on epithelial may be necessary for CD97–DAF interactions. For instance, our studies define a relative importance for the SCR-3 domain of DAF (Fig. 6). Recent work with epithelial DAF has suggested that a close extracellular spatial interaction exists between DAF SCR-3 and ICAM-1, and that such an association may limit accessibility to DAF SCR-3 (48). However, this is unlikely because we have reported previously that in unmodulated epithelia (such as those used here), ICAM-1 is either absent or expressed at very low levels (5, 49). Third, and more likely, other DAF ligands may exist. Our studies with CHO transfectants suggested a relative importance of SCR-3 in epithelial DAF interactions with PMN, and as alluded to in previous paragraphs, others have shown that SCR-1 is likely most important for CD97 interactions (41). As such, additional work will be necessary to define details of this interaction and/or the existence of additional DAF ligands expressed on PMN.

Studies directed at identifying OE-1 epitopes revealed that cells expressing truncations of DAF SCR domain 3 did

not bind OE-1, suggesting that this mAb recognizes SCR-3 and presumably, that SCR-3 is critical for PMN–DAF interactions. In addition, phage display identified a functional peptide (EVEHWYRSG) corresponding to the OE-1 binding site with a core consensus EXEX\*WXXX\*\* (where X is neutral, X\* is large and X\*\* is hydrophobic). The peptide mimetic used here (amino acid sequence EVEHWYRSG) bound to the surface of PMN, blocked both antibody binding to DAF (Western blot and ELISA), and inhibited transmigration functional responses mediated by epithelial DAF. Consistent with our findings that the OE-1 mAb recognizes a conformationally constrained epitope (e.g., OE-1 does not Western blot reduced DAF), this consensus peptide sequence does not exist in the primary structure of DAF. This is not surprising because phage can also recognize complex, discontinuous epitopes (18). Our attempts to define conformational epitopes corresponding to the OE-1 binding site using a disulfide-constrained 10-mer library resulted in no specific phage amplification or selection (unpublished data), suggesting that the OE-1 peptide represents a discontinuous epitope on DAF. Again, this is not surprising given the complex structure of membrane DAF. The four SCR domains are connected in series with each domain bearing two loops interconnected by two disulfide bonds (20). Although we do not know the exact mechanism by which this peptide mimetic functions to modulate PMN–epithelial interactions, we presume that binding to a conformational ligand on PMN occupies a site important for PMN binding to DAF SCR-3. Alternatively, this peptide could act indirectly through interactions with an accessory molecule important in DAF SCR-3 function (e.g., ICAM-1). For the reasons stated, and evidence that ICAM-1 has minimal influences on PMN–epithelial interactions without preexposure to proinflammatory stimuli (e.g., IFN- $\gamma$ , pathogenic bacteria; references 4, 5), this latter example is not likely to contribute significantly to our observations here.

In conclusion, we demonstrate here that epithelial DAF represents an apical ligand for PMN during transmigration. Moreover, these studies identify a peptide mimetic with potential in disruption of this natural epithelial–PMN interaction. Such insights offer hope in potential therapeutic development for inflammatory conditions. For example, surfaces lined by columnar epithelial cells (e.g., those of the airway and intestine) offer a potential advantage for therapy in that these surfaces are directly and immediately available for topical rather than systemic administration of locally active therapeutic compounds. It is known that transepithelial migration of PMN often parallels the degree of patient illness during acute inflammatory events. For example, interactions of PMN with the apical membrane of intestinal crypt cells likely have specific influences on epithelial ion transport; yet to interface with this apical membrane domain, transepithelial migration is required. Similarly, a variety of cytokine-specific effects on PMN–epithelial interactions likely modulate the biological sequelae of PMN–epithelial interactions postvascular emigration. The findings reported here raise the possibility that delivery of luminal

therapeutic compounds targeted to DAF-based PMN–epithelial recognition sites might represent a future avenue for local, site-specific, and nonsystemic interventions in inflammatory disorders involving selected mucosal sites.

The authors wish to acknowledge technical assistance provided by S. Burst, M. Morrissey, and R. Cotta.

This work was supported by National Institutes of Health grants HL54229, DK50189, and DE13499 and by a grant from the Crohn's and Colitis Foundation of America.

Submitted: 10 March 2003

Revised: 22 July 2003

Accepted: 22 July 2003

## References

- Parkos, C.A. 1997. Molecular events in neutrophil transepithelial migration. *Bioessays*. 19:865–873.
- Liu, Y., H.J. Buhning, K. Zen, S.L. Burst, F.J. Schnell, I.R. Williams, and C.A. Parkos. 2002. Signal regulatory protein (SIRP $\alpha$ ), a cellular ligand for CD47, regulates neutrophil transmigration. *J. Biol. Chem.* 277:10028–10036.
- Madara, J.L. 1997. Review article: pathobiology of neutrophil interactions with intestinal epithelia. *Aliment Pharmacol. Ther.* 3:57–62; discussion 62–53.
- Huang, G.T., L. Eckmann, T.C. Savidge, and M.F. Kagnoff. 1996. Infection of human intestinal epithelial cells with invasive bacteria upregulates apical intercellular adhesion molecule-1 (ICAM)-1 expression and neutrophil adhesion. *J. Clin. Invest.* 98:572–583.
- Parkos, C.A., S.P. Colgan, M.S. Diamond, A. Nusrat, T. Liang, T.A. Springer, and J.L. Madara. 1996. Expression and polarization of intercellular adhesion molecule-1 on human intestinal epithelia: consequences for CD11b/18-mediated interactions with neutrophils. *Mol. Med.* 2:489–505.
- Reaves, T.A., S.P. Colgan, P. Selvaraj, M.M. Pochet, S. Walsh, A. Nusrat, T.W. Liang, J.L. Madara, and C.A. Parkos. 2001. Neutrophil transepithelial migration: regulation at the apical epithelial surface by Fc-mediated events. *Am. J. Physiol. Gastrointest. Liver Physiol.* 280:G746–G754.
- Kirkitadze, M.D., and P.N. Barlow. 2001. Structure and flexibility of the multiple domain proteins that regulate complement activation. *Immunol. Rev.* 180:146–161.
- Turner, J.R., B.K. Rill, S.L. Carlson, D. Carnes, R. Kerner, R.J. Mrsny, and J.L. Madara. 1997. Physiological regulation of epithelial tight junctions is associated with myosin light-chain phosphorylation. *Am. J. Physiol.* 273:C1378–C1385.
- Madianos, P.N., P.N. Papapanou, U. Nannmark, G. Dahlen, and J. Sandros. 1996. Porphyromonas gingivalis FDC381 multiplies and persists within human oral epithelial cells in vitro. *Infect. Immun.* 64:660–664.
- Dharmasathaphorn, K., and J.L. Madara. 1990. Established intestinal cell lines as model systems for electrolyte transport studies. *Methods Enzymol.* 192:354–389.
- Collard, C.D., K.A. Park, M.C. Montalto, S. Alipati, J.A. Buras, G.L. Stahl, and S.P. Colgan. 2002. Neutrophil-derived glutamate regulates vascular endothelial barrier function. *J. Biol. Chem.* 2002:14801–14811.
- Dickson, M.A., W.C. Hahn, Y. Ino, V. Ronfard, J.Y. Wu, R.A. Weinberg, D.N. Louis, F.P. Li, and J.G. Rheinwald. 2000. Human keratinocytes that express hTERT and also bypass a p16(INK4a)-enforced mechanism that limits life span become immortal yet retain normal growth and differentiation characteristics. *Mol. Cell. Biol.* 20:1436–1447.
- Henson, P., and Z.G. Oades. 1975. Stimulation of human neutrophils by soluble and insoluble immunoglobulin aggregates. *J. Clin. Invest.* 56:1053–1061.
- Parkos, C.A., S.P. Colgan, A. Liang, A. Nusrat, A.E. Bacarra, D.K. Carnes, and J.L. Madara. 1996. CD 47 mediates post-adhesive events required for neutrophil migration across polarized intestinal epithelia. *J. Cell Biol.* 132:437–450.
- Parkos, C.A., C. Delp, M.A. Arnaout, and J.L. Madara. 1991. Neutrophil migration across a cultured intestinal epithelium: Dependence on a CD11b/CD18-mediated event and enhanced efficiency in the physiologic direction. *J. Clin. Invest.* 88:1605–1612.
- Colgan, S.P., C.A. Parkos, C. Delp, M.A. Arnaout, and J.L. Madara. 1993. Neutrophil migration across cultured intestinal epithelial monolayers is modulated by epithelial exposure to interferon- $\gamma$  in a highly polarized fashion. *J. Cell Biol.* 120:785–795.
- Zünd, G., S. Uezono, G.L. Stahl, A.L. Dzuz, F.X. McGowan, P.R. Hickey, and S.P. Colgan. 1997. Hypoxia enhances endotoxin-stimulated induction of functional intercellular adhesion molecule-1 (ICAM-1). *Am. J. Physiol.* 273:C1571–C1580.
- Burritt, J.B., S.C. Busse, D. Gizachew, D.W. Siemsen, M.T. Quinn, C.W. Bond, E.A. Dratz, and A.J. Jesaitis. 1998. Antibody imprint of a membrane protein surface. Phagocyte flavocytochrome b. *J. Biol. Chem.* 273:24847–24852.
- Mazzucchelli, L., J.B. Burritt, A.J. Jesaitis, A. Nusrat, T.W. Liang, A.T. Gewirtz, F.J. Schnell, and C.A. Parkos. 1999. Cell-specific peptide binding by human neutrophils. *Blood*. 93:1738–1748.
- Nicholson-Weller, A., and C.E. Wang. 1994. Structure and function of decay accelerating factor CD55. *J. Lab. Clin. Med.* 123:485–491.
- Lisanti, M.P., A. Le Bivic, A.R. Saltiel, and E. Rodriguez-Boulan. 1990. Preferred apical distribution of glycosyl-phosphatidylinositol (GPI) anchored proteins: a highly conserved feature of the polarized epithelial cell phenotype. *J. Membr. Biol.* 113:155–167.
- Liu, Y., D. Merlin, S.L. Burst, M. Pochet, J.L. Madara, and C.A. Parkos. 2001. The role of CD47 in neutrophil transmigration: Increased rate of migration correlates with increased cell surface expression of CD47. *J. Biol. Chem.* 276:40156–40166.
- Coyne, K.E., S.E. Hall, S. Thompson, M.A. Arce, T. Kinoshita, T. Fujita, D.J. Anstee, W. Rosse, and D.M. Lublin. 1992. Mapping of epitopes, glycosylation sites, and complement regulatory domains in human decay accelerating factor. *J. Immunol.* 149:2906–2913.
- Jaye, D.L., and C.A. Parkos. 2000. Neutrophil migration across intestinal epithelium. *Ann. NY Acad. Sci.* 915:151–161.
- Colgan, S.P., K.M. Comerford, and D.W. Lawrence. 2002. Epithelial cell–neutrophil interactions; a complex dialog in mucosal surveillance and inflammation. *Scientific World Journal*. 2:76–88.
- Madianos, P.N., P.N. Papapanou, and J. Sandros. 1997. Porphyromonas gingivalis infection of oral epithelium inhibits neutrophil transepithelial migration. *Infect. Immun.* 65:3983–3990.
- Colgan, S.P., A.L. Dzuz, and C.A. Parkos. 1996. Epithelial exposure to hypoxia modulates neutrophil transepithelial migration. *J. Exp. Med.* 184:1003–1015.

28. Balsam, L.B., T.W. Liang, and C.A. Parkos. 1998. Functional mapping of CD11b/CD18 epitopes important in neutrophil-epithelial interactions: a central role of the I domain. *J. Immunol.* 160:5058–5065.
29. Lea, S. 2001. Interactions of CD55 with non-complement ligands. *Biochem. Soc. Trans.* 30:1014–1019.
30. King, P.D., A.H. Batchelor, P. Lawlor, and D.R. Katz. 1990. The role of CD44, CD45, CD45RO, CD46 and CD55 as potential anti-adhesion molecules involved in the binding of human tonsillar T cells to phorbol 12-myristate 13-acetate-differentiated U-937 cells. *Eur. J. Immunol.* 20:363–368.
31. Verbakel, C.A., S. Van Duikeren, R.W. De Bruin, R.L. Marquet, and J.N. IJzermans. 2003. Human decay-accelerating factor expressed on rat hearts inhibits leukocyte adhesion. *Transpl. Int.* 16:168–172.
32. Ardman, B., M.A. Sikorski, and D.E. Staunton. 1992. CD43 interferes with T-lymphocyte adhesion. *Proc. Natl. Acad. Sci. USA.* 89:5001–5005.
33. Fanales-Belasio, E., G. Zambruno, A. Cavani, and G. Girolomoni. 1997. Antibodies against sialophorin (CD43) enhance the capacity of dendritic cells to cluster and activate T lymphocytes. *J. Immunol.* 159:2203–2211.
34. Alon, R., and S. Feigelson. 2002. From rolling to arrest on blood vessels: leukocyte tap dancing on endothelial integrin ligands and chemokines at sub-second contacts. *Semin. Immunol.* 14:93–104.
35. Detmers, P.A., and S.D. Wright. 1988. Adhesion-promoting receptors on leukocytes. *Curr. Opin. Immunol.* 1:10–15.
36. Kucik, D.F. 2002. Rearrangement of integrins in avidity regulation by leukocytes. *Immunol. Res.* 26:199–206.
37. Stewart, M., and N. Hogg. 1996. Regulation of leukocyte integrin function: affinity vs. avidity. *J. Cell. Biochem.* 61:554–561.
38. Hendeby, B., C.B. Klee, and F.R. Maxfield. 1992. Inhibition of neutrophil chemokinesis on vitronectin by inhibitors of calcineurin. *Science.* 258:296–299.
39. Cant, C.A., and A. Ullrich. 2001. Signal regulation by family conspiracy. *Cell. Mol. Life Sci.* 58:117–124.
40. Brown, E.J., and W.A. Frazier. 2001. Integrin-associated protein (CD47) and its ligands. *Trends Cell Biol.* 11:130–135.
41. Hamann, J., B. Vogel, G.M. van Schijndel, and R.A. van Lier. 1996. The seven-span transmembrane receptor CD97 has a cellular ligand (CD55, DAF). *J. Exp. Med.* 184:1185–1189.
42. Hamann, J., C. Stortelers, E. Kiss-Toth, B. Vogel, W. Eichler, and R.A. van Lier. 1998. Characterization of the CD55 (DAF)-binding site on the seven-span transmembrane receptor CD97. *Eur. J. Immunol.* 28:1701–1707.
43. Qian, Y.M., M. Haino, K. Kelly, and W.C. Song. 1999. Structural characterization of mouse CD97 and study of its specific interaction with the murine decay-accelerating factor (DAF, CD55). *Immunology.* 98:303–311.
44. Hamann, J., J.O. Wishaupt, R.A. van Lier, T.J. Smeets, F.C. Breedveld, and P.P. Tak. 1999. Expression of the activation antigen CD97 and its ligand CD55 in rheumatoid synovial tissue. *Arthritis Rheum.* 42:650–658.
45. Visser, L., A.F. de Vos, J. Hamann, M.J. Melief, M. van Meurs, R.A. van Lier, J.D. Laman, and R.Q. Hintzen. 2002. Expression of the EGF-TM7 receptor CD97 and its ligand CD55 (DAF) in multiple sclerosis. *J. Neuroimmunol.* 132:156–163.
46. Miwa, T., M.A. Maldonado, L. Zhou, X. Sun, H.Y. Luo, D. Cai, V.P. Werth, M.P. Madaio, R.A. Eisenberg, and W.C. Song. 2002. Deletion of decay-accelerating factor (CD55) exacerbates autoimmune disease development in MRL/lpr mice. *Am. J. Pathol.* 161:1077–1086.
47. Lin, H.H., M. Stacey, C. Saxby, V. Knott, Y. Chaudhry, D. Evans, S. Gordon, A.J. McKnight, P. Handford, and S. Lea. 2001. Molecular analysis of the epidermal growth factor-like short consensus repeat domain-mediated protein-protein interactions: dissection of the CD97-CD55 complex. *J. Biol. Chem.* 276:24160–24169.
48. Shafren, D.R., D.J. Dorahy, R.F. Thorne, and R.D. Barry. 2001. Cytoplasmic interactions between decay-accelerating factor and intercellular adhesion molecule-1 are not required for coxsackievirus A21 cell infection. *J. Gen. Virol.* 81:889–894.
49. Colgan, S.P., C.A. Parkos, J.B. Matthews, L. D'Andrea, C.S. Awtrey, A. Lichtman, C. Delp, and J.L. Madara. 1994. Interferon- $\gamma$  induces a surface phenotype switch in intestinal epithelia: downregulation of ion transport and upregulation of immune accessory ligands. *Am. J. Physiol.* 267:C402–C410.